Antiviral Research 170 (2019) 104564

Contents lists available at ScienceDirect

Antiviral Research

journal homepage: www.elsevier.com/locate/antiviral

Rapid isolation of a potent human antibody against H7N9 influenza virus from an infected patient

Junxin Li[a,b,1], Yang Yang[c,1], Min Wang[d,1], Xiaohu Ren[e], Zheng Yang[f], Lvyan Liu[a], Guizhong Zhang[a], Qian Chen[a,b], Wei Yang[g], Youhai H. Chen[h], Xiaochun Wan[a,*]

[a] Shenzhen Laboratory of Human Antibody Engineering, Institute of Biomedicine and Biotechnology, Shenzhen Institutes of Advanced Technology, Chinese Academy of Sciences, 1068 Xueyuan Boulevard, University City of Shenzhen, Xili Nanshan, Shenzhen, 518055, China
[b] School of Life Sciences, University of Chinese Academy of Sciences, No.19 (A) Yuquan Road, Shijingshan District, Beijing, 100049, PR China
[c] Shenzhen Key Laboratory of Pathogen and Immunity, Guangdong Key Laboratory for Diagnosis and Treatment of Emerging Infectious Diseases, State Key Discipline of Infectious Disease, Second Hospital Affiliated to Southern University of Science and Technology, Shenzhen Third People's Hospital, Shenzhen, 518112, China
[d] CAS Key Laboratory of Pathogenic Microbiology and Immunology, Institute of Microbiology, Chinese Academy of Sciences, No. 1 West Beichen Road, Beijing, 100101, China
[e] Institute of Toxicology, Shenzhen Center for Disease Control and Prevention, No 8 Longyuan Road, Nanshan District, Shenzhen, 518055, China
[f] Shenzhen Center for Chronic Disease Control, No.2021 Buxin Road, Luohu District, Shenzhen, 51822, China
[g] Savaid Medical School, University of Chinese Academy of Sciences, Beijing, China
[h] Department of Pathology and Laboratory Medicine, University of Pennsylvania School of Medicine, Philadelphia, PA, 19104, USA

ARTICLE INFO

Keywords:
Switched memory B cells
Human monoclonal antibody
H7N9
ADCC
Mass spectroscopy
Antigenic site A

ABSTRACT

Influenza virus A H7N9 remains a serious threat to public health due to the lack of effective vaccines and drugs. In this study, a neutralizing human antibody named 3L11 was rapidly isolated from the switched memory B cells of a patient infected with H7N9. The antibody 3L11 was encoded by the heavy-chain *VH1-8* gene and the light-chain *VL2-13* gene that had undergone somatic mutations, and conferred high affinity binding to H7N9 hemagglutinins (HAs). It promoted killing of infected cells by antibody-dependent cell-mediated cytotoxicity (ADCC). Epitope mapping by mass spectroscopy (MS) indicated that 3L11 bound to the peptide 149–175 of HAs that contained the 150-loop of the receptor-binding site (RBS). Additionally, the 3L11 escape strains had G151R (Gly^{151}→Arg^{151}) and S152P (Ser^{152}→Pro^{152}) mutations within a conserved antigenic site A near the RBS that were not observed in field strains. Importantly, 3L11 fully protected mice against a lethal H7N9 virus challenge, in both pre- and postexposure administration regimens. Altogether, this work demonstrates the feasibility of rapid isolation of neutralizing H7N9 antibodies from infected patients and provides a potential prophylactic and therapeutic agent against H7N9 viruses.

1. Introduction

Human infection with H7N9 avian influenza virus was first reported on 31 March 2013 in China. As of 05 September 2018, a total of 1567 cases of human infection with H7N9 virus including at least 615 deaths with a case fatality rate of 39%, have been reported by the World Health Organization (WHO). Moreover, the number of human infections and the geographical distribution of human cases in the fifth epidemic wave that occurred from 2016 to 2017 were greater than in all earlier waves (Quan et al., 2018). Additionally, since the H7N9 virus containing the S31N mutation in the M2 protein is resistant to the M2 ion channel blockers (Rimantadine and Adamantanes) (Gao et al., 2013), neuraminidase inhibitors (NAIs) such as Oseltamivir and Zanamivir have been used as the first-line antiviral drugs. Unfortunately,

Abbreviations: HA, hemagglutinin; MS, mass spectroscopy; RBS, receptor-binding site; ADCC, antibody-dependent cell-mediated cytotoxicity; NAIs, neuraminidase inhibitors; HmAbs, human monoclonal antibodies; bnAb, broadly-neutralizing antibody; BSL-3, Biosafety Level 3; AH1, A/Anhui/1/2013 (H7N9 virus); SH2, A/Shanghai/2/2013; SH1, A/Shanghai/1/2013; SZ4, A/Shenzhen/Th004/2017; HZ1, A/Hangzhou/1/2013; MDCK, Madin-Darby canine kidney; $TCID_{50}$, 50% tissue culture infective dose; UCA, unmutated common ancestor; NP, nuclear protein; IC_{50}, half maximal inhibitory concentration; BLI, bio-layer interferometry; HI, hemagglutination inhibition; LD_{50}, median lethal dose; SPF, specific-pathogen-free; MN, Microneutralization; IFA, indirect immunofluorescent assay; LDH, lactate dehydrogenase; AA, amino acid; mt3L11, mutant 3L11 antibody; wtHA, wild type hemagglutinin; mtHA, mutant hemagglutinin; NS, no significance

* Corresponding author.
E-mail address: xc.wan@siat.ac.cn (X. Wan).
[1] These authors contributed equally to this work.

https://doi.org/10.1016/j.antiviral.2019.104564
Received 11 February 2019; Received in revised form 16 July 2019; Accepted 19 July 2019
Available online 20 July 2019

previous studies have shown that the R292K mutation in the NA protein of the H7N9 virus conferred resistance to Oseltamivir and Zanamivir (Wu et al., 2013; Yen et al., 2013). In light of the above factors, H7N9 influenza is now considered a serious pandemic threat emphasizing that new and effective therapeutic measures in both the human and animal health sectors are crucial (Subbarao, 2018).

Human monoclonal antibodies (HmAbs) are being developed as alternatives to prevent and treat influenza viruses (Corti et al., 2011; Ekiert et al., 2009; Kallewaard et al., 2016; Koszalka et al., 2017; Lang et al., 2017; Marjuki et al., 2016; Pappas et al., 2014; Sui et al., 2009; Tharakaraman et al., 2015; Wu et al., 2015; Yamayoshi et al., 2017; Yu et al., 2017). The HA of the influenza virus is an envelope glycoprotein composed of two subunits, HA1 and HA2, linked by a single disulfide bond (Wilson et al., 1981). HA2 and the N- and C-terminal regions of HA1 form the highly conserved, membrane-proximal stem. Stem-specific antibodies can broadly neutralize influenza virus by inhibiting the fusion of viral and host cellular membranes (Corti et al., 2011; Ekiert et al., 2009; Kallewaard et al., 2016; Lang et al., 2017; Pappas et al., 2014; Sui et al., 2009; Tharakaraman et al., 2015; Wu et al., 2015). Unfortunately, a broadly neutralizing antibody (bnAb) targets a stem residue D^{19} (Asp^{19}) that is prone to antigenic drift and that loses efficacy against one of the circulating H7N9 outbreak viruses (A/Wuxi/1/2013) (Tharakaraman et al., 2014). This suggests that strategies that focus on development of stem-specific antibodies might not be ideal in eliciting full spectrum protection. In addition, a cocktail of antibodies recognizing distinct regions of the antigen with nonoverlapping epitopes can provide greater protective efficacy against antigenically evolving influenza viruses (Prabakaran et al., 2009).

The HA head region containing the HA1 protein possesses several variable immunodominant regions and the conserved RBS consisting of the secondary elements 130-loop, 150-loop, 190-helix, and 220-loop. RBS is an ideal target for subtype-specific broad neutralizing antibodies due to its important role in viral invasion (Hu et al., 2012; Huang et al., 2019). Previous H7N9 virus-neutralizing antibodies were considered to target an essential residue L^{226} (Leu^{226}) of the RBS (Chen et al., 2015, 2018; Wang et al., 2015). However, unlike H5N1 and H3N2 (Herfst et al., 2012; Rogers et al., 1983), increasing numbers of reports have indicated that the Q226L (Gln^{226}→Leu^{226}) substitution was not responsible for the avian-to-human receptor-binding switch for H7 HA (Shi et al., 2013; Watanabe et al., 2014; Xu et al., 2013) and therefore was prone to escape. Additionally, anti-RBS antibodies that block the interactions between HA and sialic acid receptors on immune cells can inhibit FcgRIIIa activation and ADCC elicitation (Cox et al., 2016). Overall, more HmAbs, especially antibodies targeting more conserved or unique regions of the HA head, are needed for alternative and adjunctive treatments for H7N9 infection.

Here we report the rapid development of a human antibody 3L11 against H7N9 viruses from cytokine-stimulated switched memory B cells, as previously described for HIV antibodies (Huang et al., 2013). In contrast to previously reported human antibodies, 3L11 was encoded by VH1-8 and VL2-13 germline loci. The antibody neutralized avian and human H7N9 virus *in vitro*, and fully protected infected mice through mechanisms likely involving ADCC. This work expands the potential antibody repertoire against influenza A virus and enables the development of a universal H7N9 vaccine and antibody therapy.

2. Materials and methods

2.1. Ethics statements

The collection of human blood was approved by the Ethics Committee of Shenzhen Third People's Hospital. Informed consent was obtained from the participant. All animal experiments were conducted at Biosafety Level 3 (BSL-3) facilities in accordance with ethical procedures and policies. The research was approved by the Wuhan Institute of Virology's Institutional Animal Care and Use Committee (Permit number WIV/A3/04/201701).

2.2. Virus and cell lines

The H7N9 viruses used in this study were A/Anhui/1/2013 (AH1), A/Shanghai/2/2013 (SH2), A/Shanghai/1/2013 (SH1) and A/Shenzhen/Th004/2017 (SZ4). Viruses were propagated in Madin-Darby canine kidney (MDCK) cells, and virus-containing supernatants were pooled, clarified by centrifugation, and stored in aliquots at −80 °C. The 50% tissue culture infective dose ($TCID_{50}$) was determined by serial titration of viruses in MDCK cells and was calculated using the method of Reed and Muench (1938). All infectious H7N9 viruses were handled in BSL-3 facilities at the Wuhan Institute of Virology, the Beijing Institute of Microbiology, Chinese Academy of Sciences and the Shenzhen Third People's Hospital.

The cell lines 293T and 293F were maintained in DMEM medium with 10% FBS and serum-free 293 expression medium (Thermo Scientific), respectively. The 3T3-CD40L cells were generated by transducing NIH-3T3 cells with human CD40L cDNA. Briefly, human CD40L cDNA was synthesized and cloned into the lentiviral expression vector pLVX-IRES-ZsGreen (Invitrogen). The pLVX-CD40L-IRES-ZsGreen plasmid was transfected with pMD2.G and psPAX2 plasmids (Addgene) into 293T cells to harvest infectious virus particles, followed by infecting NIH-3T3 cells.

The Chinese hamster ovary cell lines (CHO–S,Thermo Scientific) were maintained in ExpiCHO™ Expression Medium (Thermo Scientific). AH1 HA gene expression vectors (pCMV-HA, Sino Biological) were introduced into CHO–S cells by a gene pulser (Bio-rad) as described previously (Cai et al., 2014). Transfected cells were cultured in selective medium containing 1.5 mg/ml G418 (Sigma) for two weeks. CHO–S cell lines constitutively expressing HA were obtained by limiting dilution.

2.3. Sample collection

Blood was obtained from a Chinese adult who had recovered from H7N9 infection. Peripheral blood mononuclear cells (PBMCs) were isolated from the blood using Ficoll-Paque (GE Healthcare). The isolated PBMCs were suspended at 1×10^7 cells per ml in CS10 freezing medium (Stemcell) and stored in a liquid nitrogen tank until use.

2.4. Production of human antibodies

Human monoclonal antibodies were isolated from PBMCs as previously described (Huang et al., 2013). Briefly, 3T3-CD40L cells were irradiated with 5000 rads in Rs2000 (RAD Source). Memory B cells from PBMCs were stained with CD19-PE-Cy7 (BD Biosciences), IgA-APC (Jackson ImmunoResearch Laboratories), IgD-FITC (BD Pharmingen), and IgM-PE (Jackson ImmunoResearch Laboratories). The $CD19^+IgM^-IgA^-IgD^-$ B cells were sorted in a FACSAria (BD Biosciences). The B cells were activated in IMDM medium (Gibco) containing IL-2 (Roche), IL-21 (Invitrogen) and 3T3-CD40L cells and incubated at 37 °C in 5% CO_2 for 13 days. Culture supernatants were tested by a neutralization assay as described below. From positive cultures, the *VH* and *VL* gene transcript sequences were retrieved by nested RT-PCR as previously described (Smith et al., 2009). Heavy-chain and light-chain DNA fused with the constant gamma 1 heavy and lambda light chain coding sequences were cloned into pcDNA 3.1 expression vectors (Invitrogen). Monoclonal antibodies were produced by transient transfection of 293F cells with vectors and PEI (Sigma-Aldrich) as described previously (Tom et al., 2008). Supernatants were collected after five days of culture and antibodies were purified by Protein A chromatography (GE Healthcare).

2.5. Recombinant proteins, expression vectors and peptides

Recombinant H7N9 HA (SH2, SH1, A/Hangzhou/1/2013 (HZ1))

and HA1 (AH1) were purchased from Acrobiosystems in China. AH1 NA gene expression vector (pCMV-NA) was purchased from Sino Biological. Peptides coupled with biotin were synthesized by the GenScript Corporation. The genes of the UCA antibody, the mutant 3L11 antibody containing L234A/L235A and the mutant SH2 HA containing G151R/S152P were synthesized and cloned into pcDNA3.1 expression vectors (Invitrogen), respectively. Proteins were produced and purified by transient transfection as described above.

2.6. Enzyme-linked immunosorbent assay (ELISA)

Fifty nanograms of recombinant HAs, HA1, or biotin-peptides were immobilized on 96-well microtiter plates (Thermo Scientific). The plates were blocked using 1% BSA (Sigma-Aldrich) and then incubated with 100 ng of antibodies for 1 h. Horseradish peroxidase-conjugated goat anti-human IgG, tetramethylbenzydine (TMB) (Sigma-Aldrich), and 1 mol/L of sulfuric acid were sequentially added in the plates. Data were recorded (at 450 nm) using an M1000 (Tecan) plate reader.

2.7. Microneutralization (MN) assay

Culture supernatants or serial dilutions of mAbs were prepared, mixed in equal volumes with 100 $TCID_{50}$ of the appropriate viruses, placed in 96-well tissue culture plates, and incubated for 1 h at 37 °C. Indicator MDCK cells (1.5×10^4 cells per well) were added to each well and incubated at 37 °C for 20 h. To establish the end point, cell monolayers were then washed with PBS and fixed in acetone, and viral antigen was detected by indirect ELISA with an mAb against influenza A nuclear protein (NP) (Millipore). Plates were developed with TMB and sulfuric acid. Data were recorded (at 450 nm) using an M1000 (Tecan) plate reader. The final concentration of antibody that reduced infection to 50% (IC_{50}) was determined using GraphPad Prism 5 software.

2.8. Antibody-dependent cell-mediated cytotoxicity (ADCC) assay

Human lung epithelial cells A549 were plated in 96 well plates in RPMI1640 medium (Hyclone) with 10% fetal bovine serum (Hyclone) to obtain a 90% confluence. After PBS washing, cells were infected with 200 $TCID_{50}$ of SH2 H7N9 virus at 37 °C for 2 h. The supernatant was then replaced with fresh RPMI1640 medium. Infected cells were cultured for 24 h in a 5% CO_2 incubator at 37 °C. Serially diluted antibodies were added and incubated for 1 h. The antibodies were replaced with 1.5×10^5 of PBMCs in 150 µl RPMI1640 medium, and the cells were incubated for 4 h. Cytotoxicity was detected using an lactate dehydrogenase (LDH) release assay (Promega). Wells containing A549 cells and lysis buffer were considered as a positive control. Wells containing PBMCs and virus-infected A549 cells were considered as a negative control. Wells containing only virus-infected A549 were considered as backgrounds. The OD492 was recorded using a microplate reader. ADCC percentage was calculated according the following equation. ADCC percentage = 100 × (OD492 sample average - OD492 negative control average)/(OD492 A549 lysis - OD492 A549 only).

CHO–S cell lines constitutively expressing HA as the target cells were seeded in each well of a 96-well flat-bottomed culture plate (2×10^4 cells/well). The cells were incubated with 5 µg/ml of antibodies for 1 h. Normal human PBMCs from two independent donors, as the effector cells (5×10^5 cells/well), were co-cultured with antibody-treated target cells at 37 °C for 4 h, respectively. Cytotoxicity was detected using an LDH release assay as described above.

2.9. KD determination

KD was determined by bio-layer interferometry (BLI) using an Octet K2 instrument (PALL ForteBio). Antibodies or peptides in SD buffer (1x PBS, pH7.4, 1% BSA, and 0.002% Tween 20 (Sigma)) were loaded onto Protein A biosensors or Streptavidin biosensors (ForteBio) and incubated with various concentrations of antigens or antibodies. All binding data were collected at 30 °C. The experiments comprised 4 steps: (1) antibodies or peptides loading onto the biosensor; (2) baseline acquisition for 60 s; (3) association of antigens or antibodies for the measurement of k_{on}; and (4) dissociation of antigens for the measurement of k_{dis}. Baseline and dissociation steps were carried out in SD buffer only. The ratio of k_{on} to k_{dis} determined the value of KD reported here.

2.10. Indirect immunofluorescent assay (IFA) and flow cytometry

The 293T cells were transfected with pCMV-HA vector or pCMV-NA control vector by PEI. At 24 h post-transfection, the cells were fixed with 4% paraformaldehyde and then permeabilized with 0.2% Triton X-100 (Sigma). Antigens were probed with antibodies followed by APC anti-human IgG Fc or PE anti-human IgG Fc (BioLegend). Binding of antibodies to cells was analyzed using a 1 × 71 inverted microscope (Olympus) and FACSCanto2 (BD Biosciences).

2.11. Hemagglutination inhibition (HI) assays

SH2 Viruses were diluted to eight hemagglutination units and incubated with an equal volume of serially diluted antibody at room temperature. An equal volume of 0.5% horse red blood cells was added to the wells, and incubation was continued on a gently rocking plate for 30 min at room temperature. Cell button formation was scored as evidence of HI.

2.12. Prophylaxis and therapy in infected mice with 3L11

To measure prophylactic efficacy, three groups of female BALB/c mice (nine mice per group; six to eight weeks old) were intraperitoneally injected with 30 mg/kg of 4E3 (human IgG1 isotype control), 10 and 30 mg/kg of 3L11 at 24 h before being challenged intranasally with 10 median lethal dose (LD_{50}) units of virus (SH2) diluted with 50 µl PBS under anesthesia with isoflurane. To test the therapeutic effect of 3L11, five groups of female BALB/c mice (nine mice per group; six to eight weeks old) were anesthetized and inoculated with 10 LD_{50} units of virus. After 24 h, mice were injected intraperitoneally with 30 mg/kg of 4E3, 10 and 30 mg/kg of 3L11 or 10 and 30 mg/kg of CT149, a neutralizing anti-stem HmAb (Wu et al., 2015). Viral loads in the lungs were measured by a $TCID_{50}$ assay on day five post infection (three mice per group). Mice were monitored daily for survival and weight loss until day 14 post-infection. Mice that lost more than 35% of their pre-infection body weight were euthanized.

2.13. Epitope mapping of 3L11 using mass spectroscopy (MS)

For epitope excision, SH2 HA protein was digested with Trypsin (Promega) at 37 °C for 12h. Epitope extraction was performed using a Pierce Crosslink Immunoprecipitation Kit (Thermo Scientific). Briefly, 10 µg of antibody was enriched by the protein A/G crosslinked with agarose in a column. The digestion products were then added to the antibody-crosslinked resin and incubated in the column for 2 h. The epitope was eluted by elution buffer with low pH and desalted by the Pierce C18 Spin (Thermo Scientific) for MS analysis using a Q Exactive LC-ESI-MS/MS system (Thermo Scientific).

2.14. Selection of escape mutants

Escape mutants were selected by culturing SH1 and SZ4 in embryonated chicken eggs in the presence of 3L11 as described previously (Webster and Laver, 1980). Briefly, viruses (10^6 $TCID_{50}$) were incubated with 3L11 (500 µg/ml) for 1 h, and the mixtures were then inoculated into the allantoic cavities of 10-day-old specific-pathogen-

free (SPF) embryonated chicken eggs. The virus yield was used for limiting dilution cloning in embryonated chicken eggs. Viral RNA was extracted using the QIAamp RNA Viral Kit (Qiagen). The RNA was reverse transcribed into single-stranded DNA with M-MuLV reverse transcriptase (New England Biolabs). The HA gene was amplified using a Phusion™ High-Fidelity PCR Kit (New England Biolabs). The PCR products were purified using a Cycle-Pure Kit and a Gel Extraction Kit (Omega Bio-Tek), and the fragments were cloned into pMD 19-T Vector (TaKaRa). The fragments were sequenced by Invitrogen Inc. and analyzed using DNAssist 2.2 software.

2.15. Statistical analysis

Data are presented as the mean ± SD (Standard Deviation). All analyses were performed using GraphPad Prism version 7.0 for Windows (GraphPad Software, San Diego California, USA). Data were subjected to statistical analysis by log-rank test (survival curves),two-way ANOVA (neutralizing activities, weight loss, ADCC activities) and *t*-test (binding activities, virus titres). The *P* values less than 0.05 were considered statistically significant.

3. Results

3.1. Characterization of human monoclonal antibodies

$CD19^+IgM^-IgA^-IgD^-$ memory B cells were sorted from PBMCs using a FACSAria (Fig. 1A). B cells were plated into 384-well plates at a density of four B cells per well, and cultured for 13 days in the presence of IL2, IL21 and 3T3-CD40L feeder cells. Fifty-eight percent of the wells produced more than 1 μg/ml IgG in the supernatants, which were used for the MN and ELISA assays. A neutralizing antibody 3L11 was isolated, and its genes were transfected into 293F cells. Transfectant cells were grown in serum-free culture, and 3L11 in the culture supernatant was purified.

The 3L11 antibody exhibited neutralizing activities against AH1 H7N9 (A/Anhui/1/2013) in a dose-dependent manner, with an IC_{50} value of 24.63 μg/ml (Fig. 1B). Sequence analysis indicated that 3L11 used a rare lineage with *VH1-8* and *VL2-13* gene segments and carried somatic mutations of 8.87% and 5.55%, respectively (Fig. 1C). Somatic mutations mainly occurred in the CDR (Complementarity Determining Region), especially in the CDR3. To assess the contribution of somatic mutations to affinity maturation, we reconstructed and produced the UCA (unmutated common ancestor) antibody, which lost reactivity against HAs as determined by ELISA analysis (Fig. 1D). Altogether, somatic mutations endowed 3L11 with the high affinity and breadth to H7 HAs.

3.2. Specificity and affinity of 3L11

To determine the binding specificity of 3L11, we expressed the viral HA and NA (neuraminidase) in 293T cells and performed the analysis using IFA and flow cytometry. As shown in Fig. 2A and B, 3L11 bound to the H7 HA rather than NA on the cell surface. To measure the affinities of the antibody, bio-layer interferometry using recombinant H7

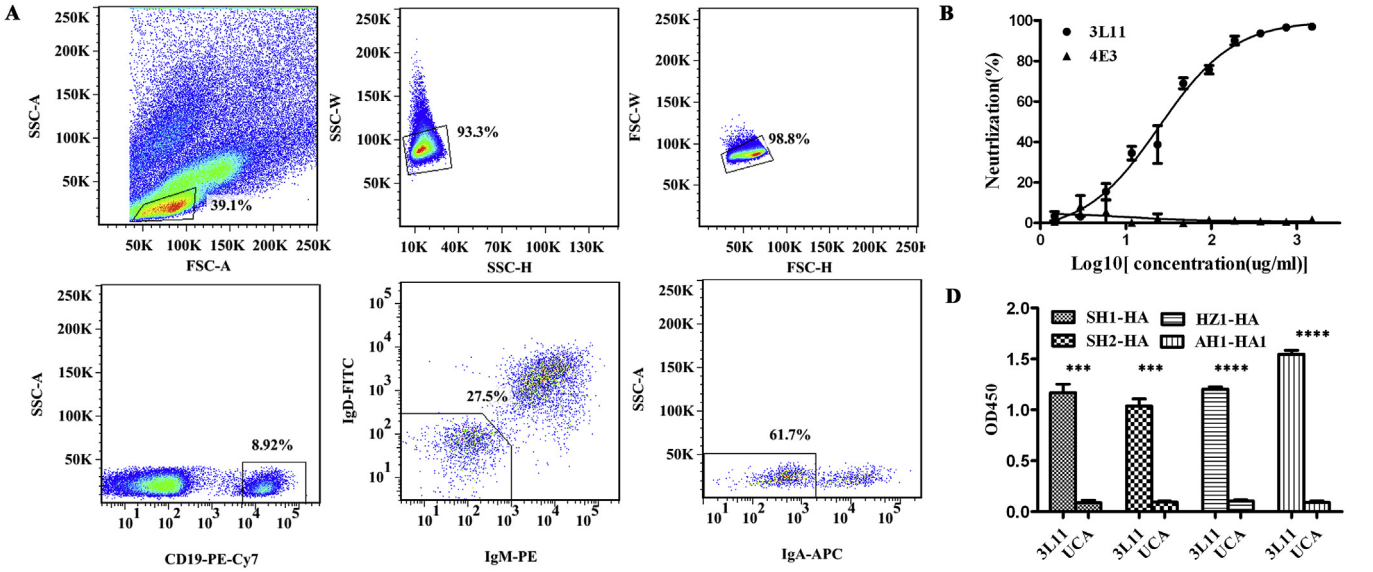

C

VH

CDR1 CDR2 CDR3

3L11 QVQLVESGAEVKKPGASVKVSCKASGYIFTSYDINWVRQATGQGLEWMGWMNPDSGDTGFAQKFQGRVTMTRNTSITTAYMELSSLTSEDTAVYYCATGNADCSGGSCYNWFDFWGQGTLVTVSS

UCA *****Q**********T*********N**N**Y**********S*********R*********R*-GY**********

VL

CDR1 CDR2 CDR3

3L11 SSELTQDPAVSVALGQTVRITCQGDRLRSYYASWYQQKPGQAPVLVIYGKNNRPSGIPDRFSGSSSGNTASLTITGAQAEDEADYYCNSRDTSG-YHLVFGGGTKLTVLV

UCA **********S********************S**NHLV**********

Fig. 1. Isolation and Characterization of 3L11.

A. $CD19^+IgM^-IgA^-IgD^-$ memory B cells (switched memory B cells) from PBMCs were sorted for isolation of neutralizing antibodies. The gating strategies of switched memory B cells are shown.

B. The neutralizing activity of 3L11 against a representative subtype H7N9 virus, A/Anhui/1/2013 (AH1), was tested by MN assay. 4E3 is an irrelevant human IgG1 antibody. Compared with the 4E3 antibody, the 3L11 antibody showed significant neutralizing activities ($P < 0.0001$). All error bars reflect SD of three replications.

C. Alignment of VH and VL amino acid sequences of 3L11 and its UCA antibody. Asterisks indicate identical residues. Amino acid substitutions are shown. Red boxes indicate CDR borders according to Kabat.

D. The binding activities of 3L11 and its UCA antibody to A/Shanghai/2/2013 (SH2) HA, A/Shanghai/1/2013 (SH1) HA, A/Hangzhou/1/2013 (HZ1) HA and AH1 HA1, were tested using ELISA. The mean OD450 values of three independent replications and error bars (SDs) are shown. ***: compared with the UCA antibody, $P < 0.001$. ****: compared with the UCA antibody, $P < 0.0001$.

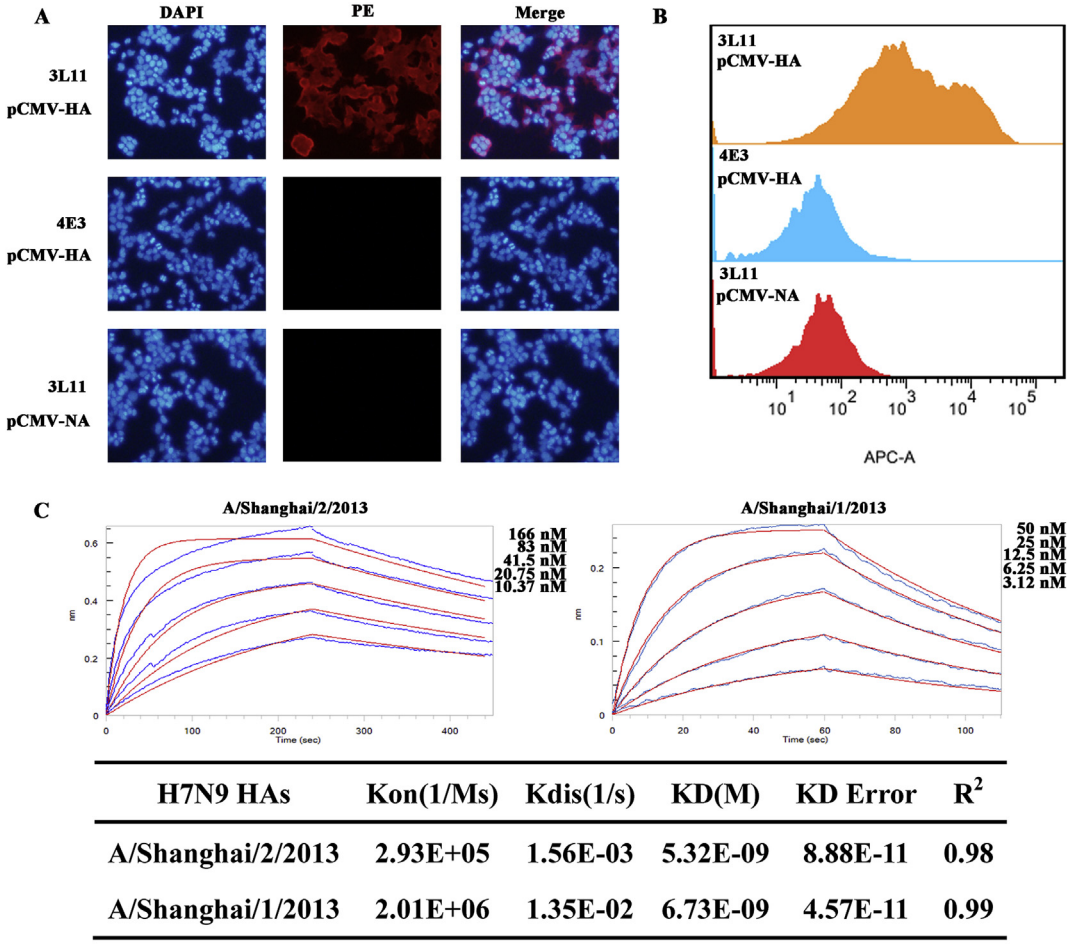

H7N9 HAs	Kon(1/Ms)	Kdis(1/s)	KD(M)	KD Error	R^2
A/Shanghai/2/2013	2.93E+05	1.56E-03	5.32E-09	8.88E-11	0.98
A/Shanghai/1/2013	2.01E+06	1.35E-02	6.73E-09	4.57E-11	0.99

Fig. 2. The binding specificity and affinity of 3L11.
A. The binding specificity of 3L11 to H7 HA was determined using IFA. Scale bar, 50 μM. HA gene and NA gene were expressed in the 293T cells and detected by IFA, respectively. Cells were immunostained for the HA (red), NA (red) and DNA (DAPI, blue).
B. The binding specificity of 3L11 to H7 HA was determined using flow cytometry. HA gene and NA gene were expressed in the 293T cells and detected by flow cytometry, respectively.
C. 3L11 was loaded onto Protein A biosensors for BLI analysis with SH2 HA and SH1 HA. Blue curves are the experimental traces obtained from bio-layer interferometry experiments, and red curves are the best global fits to the data used to calculate the values of Kon, Kdis and KD.

HAs was performed. Fig. 2C shows the association and dissociation curve of 3L11 at the indicated concentrations of HAs. Based on the curve, 3L11 showed similar binding affinities for SH1 HA (containing the avian-signature residue Gln^{226}) and SH2 HA (containing the human-signature residue Leu^{226}), with KD values of 6.73×10^{-9} and 5.32×10^{-9}, respectively. In this context, it is plausible that 3L11 does not contact the four residues in the RBS, i.e., 138AA (amino acid), 186AA, 221AA, and 226AA (Shi et al., 2013).

3.3. Protection efficacy of 3L11 in vivo

For *in vivo* protection studies, we chose A/Shanghai/2/2013 as a representative virus from the H7N9 subclade. A dose of 10 LD_{50} was chosen to ensure 100% mortality in the isotype control group (4E3).

To assess the prophylactic efficacy of 3L11, BALB/c mice were treated with two different doses of antibody at 24 h before virus challenge. As shown in Fig. 3A and B, mice in the control group ($n = 6$) all died 11 days after viral challenge with severe weight loss. In contrast, 3L11 at 10 and 30 mg/kg ($n = 6$ per group) conferred full protection (100% survival rate) from lethality by H7N9 in the infected mice without weight loss. To verify that the protection of the infected mice was due to the inhibition of viral proliferation, viral dissemination in the lungs was determined. As shown in Fig. 3E, mice ($n = 3$) receiving 4E3 showed a high titer of virus (3160 $TCID_{50}$/ml) in the lungs at five days post infection. In contrast, after passive immunization with either 10 mg/kg or 30 mg/kg of 3L11, viral proliferation was noticeably inhibited, and the virus was undetectable in the mice. Taken together, these results indicate that 3L11 can be highly effective as a prophylactic modality in mice against H7N9 infection and disease.

Next, we evaluated the therapeutic activity of 3L11 against H7N9 infection. As shown in Fig. 3C, full protection (100% survival rate) was observed when mice were treated with 30 mg/kg 3L11 ($n = 6$) at 24 h after virus challenge. A single treatment of 10 mg/kg of 3L11 ($n = 6$) in mice provided 83% protection (83% survival rate). Although mice receiving 3L11 at 30 mg/kg showed weight loss after infection, body weight started to recover after five days, and the mice returned to their starting weight by the study's end (Fig. 3D). Mice receiving 3L11 at 10 mg/kg lost approximately 20% of body weight until day 7 before starting to recover, suggesting that the health of the infected mice was also substantially improved. Importantly, the virus was also undetectable in infected mice treated with 3L11 at 10 and 30 mg/kg at five days post infection (Fig. 3F). Compared with 3L11, mice receiving CT149, a broad neutralizing HumAb, exhibited more severe weight loss (both 10 mg/kg and 30 mg/kg groups, $P < 0.05$), as shown in Fig. 3D. It demonstrated 50% (10 mg/kg group, $P = 0.18$) and 66% (30 mg/kg group, $P = 0.13$) protection to H7N9-infected mice which showed the

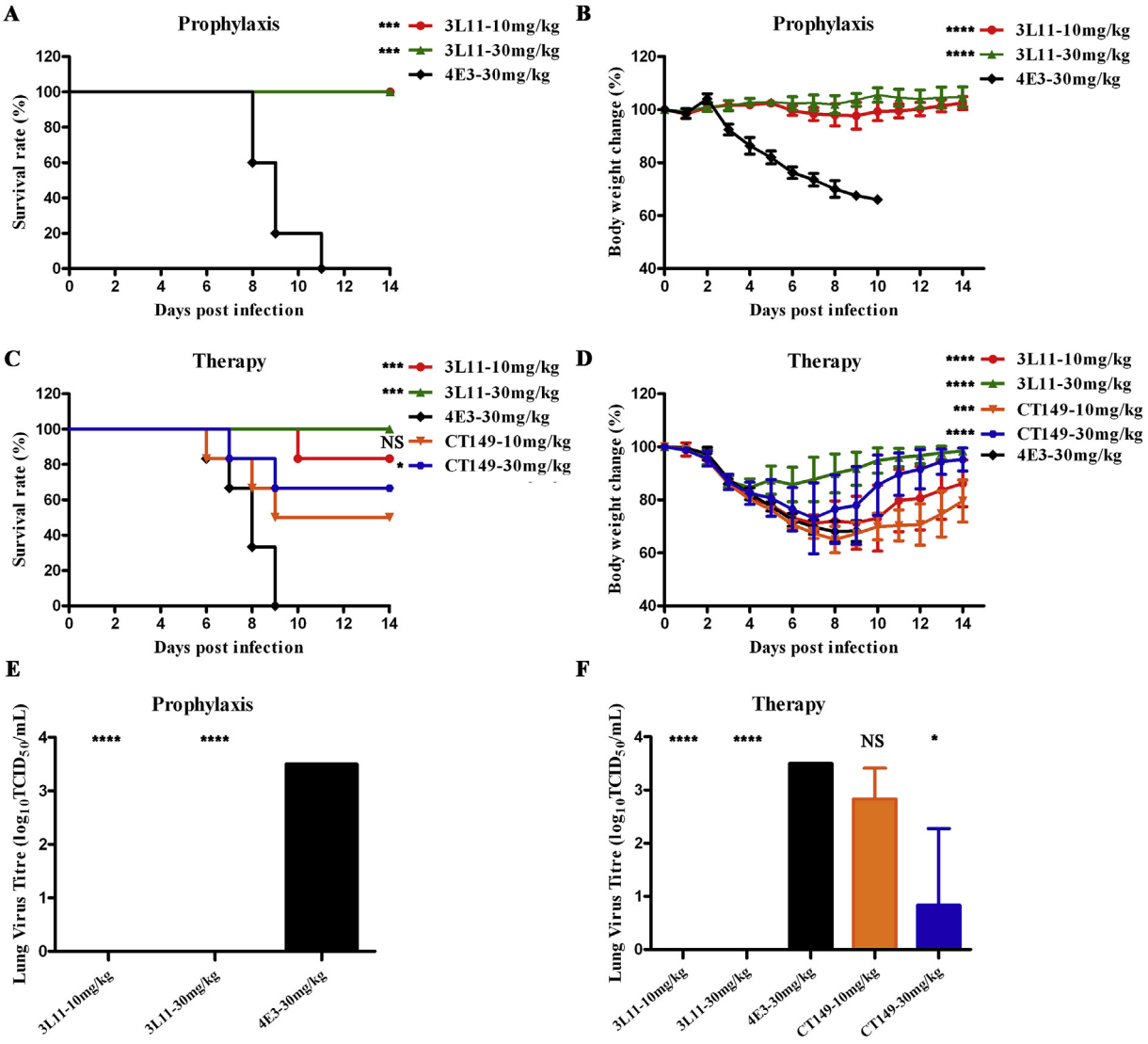

Fig. 3. Prophylactic and Therapeutic efficacy of 3L11 in mice. For the prophylactic efficacy study, mice were treated with mAbs 24 h before viral challenge and were monitored daily for 14 days for the accumulated mortality. (A), weight loss (B) and lung virus titres (E). For the therapeutic efficacy study, mice were treated with mAbs 24 h after viral challenge and were monitored daily for 14 days for the accumulated mortality (C), weight loss (D) and lung virus titres (F). The weight loss (B and D, 6 mice per group) and lung virus titres (E and F, 3 mice per group) represent means per group with SDs. *: compared with the 4E3 antibody, $P < 0.05$. ***: compared with the 4E3 antibody, $P < 0.001$. ****: compared with the 4E3 antibody, $P < 0.0001$. NS: no significance.

virus titers of 1264 $TCID_{50}$/ml ($P < 0.01$) and 105 $TCID_{50}$/ml ($P = 0.37$), respectively, in the lungs at five days post infection (Fig. 3C and F).

3.4. Epitope mapping

First, we determined using ELISA that 3L11 bound to the H7 HA1 protein (Fig. 1D) forming a globular HA head domain. Moreover, because 3L11 exhibited relatively weak HI activity with a titer of 50 μg/ml (Fig. 4A), it was possible that 3L11 bound to the area near the RBS, and thus effected its recognition and interaction with the human cellular receptors by steric hindrance (Xiong et al., 2015). To further investigate the binding site of 3L11, SH2 HA protein was digested with trypsin, and peptides were immunoprecipitated by 3L11 for MS analysis. As expected, the results showed that a peptide bound to 3L11. The molecular mass of the peptide was in good agreement with the theoretical average molecular mass of the peptide 149–175 of HA (RSGSSFYAEMKWLLSNTDNAAFPQMTK; 3080 Da) (Fig. 4B). The binding affinity of 3L11 and the peptide was 2.28×10^{-7} M (Fig. 4C). Amino acids WLLSNTDNAAFPQ in the peptide 149–175 constitute the 150-loop (Fig. 4D), which is a unique structure of the H7N9 RBS that influences the orientation of how the human receptor binds to human H7N9 HA (Xiong et al., 2013).

To further examine the binding residues, we tried to generate escape mutants of SH1 and SZ4 virus under the pressure of 3L11. By co-culture mixture of virus and 3L11 in the allantoic cavity of chick embryos, we obtained four escape mutants that were not neutralized by 500 μg/ml of 3L11. By direct sequencing, we found that escape mutants possessed G151R and S152P or G151K and S152P substitutions in the peptide 149–175 of HA (Table 1), which was consistent with the findings of the MS analysis. Moreover, we produced the mutant SH2 HA containing G151R and S152P that was unable to bind to the 3L11 antibody (Supplementary Fig. 1). The mutations were located upstream of the 150-loop and were not involved in the RBS (Fig. 4D). To determine whether the mutations had emerged in field strains, we compared amino acid sequences of the 3L11 escape strains with all available H7N9 virus sequences in the GenBank database and the GISAID database using DNAssist 2.2. The alignment result indicated that the mutations of G151R/S152P or G151K/S152P were not previously observed in field strains. Thus, it is plausible that 3L11 can neutralize all subclades of H7N9 virus that have previously emerged.

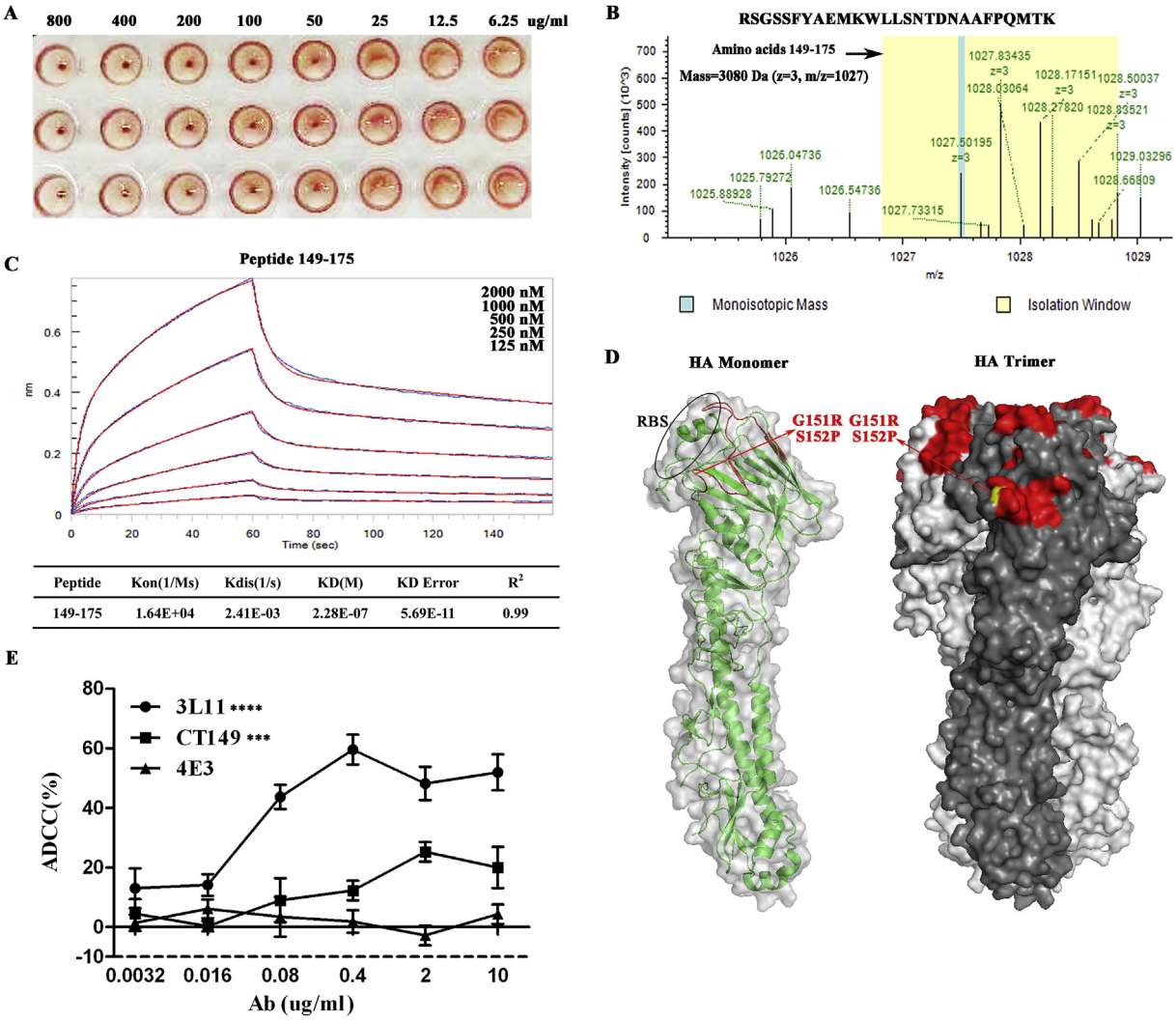

Peptide	Kon(1/Ms)	Kdis(1/s)	KD(M)	KD Error	R^2
149-175	1.64E+04	2.41E-03	2.28E-07	5.69E-11	0.99

Fig. 4. Epitope mapping of 3L11 using MS and escape mutants.
A. Hemagglutinin inhibition (HI) assay. Cell button formation was scored as evidence of HI. The influenza virus was blocked from causing hemagglutination by the 3L11 antibody. The HI titer is the last diluted concentration (50 μg/ml) of 3L11 showing completely inhibited hemagglutination.
B. Mass spectrometric characterization of the peptide. The spectrum shows the isotopic patterns of peptide precursors of 3L11 in the yellow isolation window. m/z is the mass to charge ratio.
C. The peptide was loaded onto SA biosensor for BLI analysis with 3L11. The calculated values of Kon, Kdis and KD are shown.
D. The peptide was labeled on SH2 HA monomer and trimer structures (PDB accession code 4LN6). Images were created using PyMOL software. The peptide 149–175 is shown in red. Amino acid mutations of G151R and S152P are shown in yellow.
E. ADCC activities on virus-infected A549 cells mediated by freshly prepared human PBMCs. All error bars reflect SD of three replications. Compared with the CT149 antibody, 3L11 exhibited more potent cytotoxicity ($P < 0.0001$). ***: compared with the 4E3 antibody, $P < 0.001$. ****: compared with the 4E3 antibody, $P < 0.0001$.

3.5. Fc-dependent activity of 3L11

Although 3L11 has lower neutralization activity (IC_{50} = 24.63 μg/ml) against H7N9 virus *in vitro* than CT149 (IC_{50} = 0.904 μg/ml)(Wu et al., 2015), 3L11 demonstrated more potent protection *in vivo* (Fig. 3C, D and 3F). Immunoglobulin Fc region-mediated effector pathways have been implicated in the protective activity of antibodies *in vivo* by engaging host effector cells in killing virus-infected cells (Terajima et al., 2011; Vanderven et al., 2017). To identify potential host-dependent antiviral functions of 3L11, we analyzed its activity in ADCC assays *in intro*. As shown in Figs. 4E and 3L11 at 400 ng/ml resulted in ~60% cytotoxicity using PBMCs as effectors, whereas CT149, a human antibody targeting the HA stem and a mediator of ADCC, achieved only ~25% cytotoxicity at 2 μg/ml. The ADCC effect of 3L11, at a concentration of 5 μg/ml, was also confirmed with CHO cells constitutively expressing AH1 HA (Supplementary Fig. 2). These data suggested that 3L11 may also depend on Fc-mediated effectors for *in vivo* protection.

4. Discussion

Rapid isolation and epitope mapping of human monoclonal antibodies against newly emerging influenza strains are important for the control of influenza pandemic and the development of vaccines. In this study, we used cytokines IL-2, IL-21, and irradiated 3T3-CD40L feeder cells to stimulate switch-memory B cells to produce high concentrations of IgG in the supernatant. The supernatant was screened by MN and the desired antibody was cloned. This protocol can be completed in two weeks. To the best of our knowledge, the influenza virus-neutralizing HmAb was isolated via this method for the first time. In addition, although X-ray analysis is probably the most precise method for epitope mapping, it is time consuming because of the difficulties associated

Table 1
Amino acid substitutions in HA of escape mutants selected by 3L11.

Escape mutants	HA[b] of allantoic fluids	the peptide 149-175
SH1-WT	ND	RSGSSFYAEMKWLLSNTDNAAFPQMTK
SH1-mt1	2^6	RS**RP**[a]SFYAEMKWLLSNTDNAAFPQMTK
SH1-mt2	2^5	RS**KP**SFYAEMKWLLSNTDNAAFPQMTK
SZ4-WT	ND	RSGSSFYAEMKWLLSNTDNAAFPQMTK
SZ4-mt1	2^5	RS**RP**SFYAEMKWLLSNTDNAAFPQMTK
SZ4-mt2	2^5	RS**RP**SFYAEMKWLLSNTDNAAFPQMTK

SH1-WT: Wild type SH1 H7N9 virus; SZ4-WT: Wild type SZ4 H7N9 virus.
SH1-mt1: the first 3L11 escape mutant of SH1 virus in an embryonated chicken egg. Other mutant strains have similar naming.
ND: Not detected.
[a] The substituted amino acids between the wild type virus and the mutant virus are labeled in bold and underlined.
[b] Hemagglutination assays were performed using serially diluted allantoic fluids.

with protein crystallization (Davies and Cohen, 1996). Therefore, to rapidly elucidate epitopes, we performed proteolytic digestion of the HA followed by immunoprecipitation with the antibody and mass spectrometric characterization of the antigenic peptides. Similar methods have been applied for the rapid characterization of linear and discontinuous epitopes of anti-HIV antibodies (Hochleitner et al., 2000; Jeyarajah et al., 1998).

In the previous reports, neutralizing HmAbs were dominated by the VH1-69 (Pappas et al., 2014), VH6-1 (Kallewaard et al., 2016), VH1-18 (Wu et al., 2015) and VH3-30 (Corti et al., 2011) antibodies. In our study, 3L11 was isolated from one patient who recovered from infection with the H7N9 virus. The 3L11 antibody was a unique neutralizing HmAb in that it was composed of the VH1-8 and VL2-13 chains with somatic mutations. As with VH1-69, the UCA (unmutated common ancestor) antibody of 3L11 also failed to bind to and neutralize the H7N9 virus. Obviously, somatic mutations and rearrangement of the *VDJ* gene segments allowed the VH1-8 antibody to gain the binding affinity and neutralizing activity against H7N9 viruses. Interestingly, a previous study showed that a small proportion of antibodies used the *VH1-8* gene to bind to the stem of H1N1 HA (Pappas et al., 2014). These findings indicated that the accumulation of multiple favorable mutations diversified antibody descendants, providing alternative solutions for binding to the selecting antigen or epitope. Therefore, VH1-8 germline antibodies could also be expected to become broadly protective antibodies through initiating affinity maturation *in vivo* or *in vitro*.

In our study, despite its low neutralization activity against H7N9 viruses *in vitro*, the *in vivo* protective efficacy of 3L11 in the mouse model was possibly mediated by the Fc-fragment of the mAb. The 3L11 antibody targeted the residues near the RBS, including G151 and S152 (all H7 numbering starting from the first methionine) upstream of the 150-loop, and thus weakly interfered with receptor binding, possibly by steric hindrance (Xiong et al., 2015). G151/S152 were located in the highly conserved antigenic site A (RRSGSS) of H7 HA (Schmeisser et al., 2015). In general (mouse) antibodies targeting antigenic site A (e.g. R149 or S150),showed high neutralization (IC_{50} = 1–3 μg/ml) and HI (a titer of 9.2–12.8 ng/ml) activities but no ADCC activity (Tan et al., 2016). By contrast, 3L11 demonstrated poor neutralization (IC_{50} = 24.63 μg/ml) and HI (a titer of 50 μg/ml) activities but potent ADCC activity (~60% cytotoxicity at 400 ng/ml of 3L11). These results are consistent with previous findings that antibodies with high HI activity are not effective at mediating ADCC due to inhibiting the interactions between HA and sialic acid receptors on the immune cells that are required for optimal FcgRIIIa activation and ADCC elicitation. Moreover, the inhibition efficiency of ADCC activity strongly correlates with the HI titer of antibodies (Cox et al., 2016). At present, vaccination regimens to protect against H7 virus often only elicit low immunogenicity in terms of HI antibodies in clinical trials (Fries et al., 2013; Mulligan et al., 2014). However, the HI assay is not be sufficient to measure the full extent of the antibody response against the H7 virus (Florian and Cox, 2013; Stadlbauer et al., 2017). Thus, when evaluating immune responses to vaccination with antigenic site A, binding but low-neutralizing or non-neutralizing antibodies should be given consideration, as these can confer protection by other mechanisms including antibody-dependent cell-mediated cytotoxicity (ADCC).

5. Conclusions

The study demonstrates that 3L11, a HA7 head-specific HmAb, can neutralize H7N9 viruses *in vitro*, and fully protect infected mice *in vivo*. This antibody may potentially be used either alone or in combination with stem-specific antibodies or with small-molecule inhibitors to treat human H7N9 cases. In addition, we defined the protective mechanism of 3L11 that could help inform the development of influenza vaccines.

Acknowledgments

This work was supported by the Shenzhen Technology Innovation Project [grant number JSGG20160229202150023]; the Project of Guangdong Scientific Plan Foundation [grant number 2013A022100037]; the Fourth Batch of Talents Project in Guangdong Province [grant number 2014-1]; the National Research Council of Science and Technology Major Project [grant number 2018ZX10101004]; the National Science and Technology Major Project [grant number 2018ZX09711003-002-001] and the National Natural Science Foundation of China [grant number 81802004]. We thank Dr. Jianjun Chen at the Wuhan Institute of Virology for the animal experiments.

Appendix A. Supplementary data

Supplementary data to this article can be found online at https://doi.org/10.1016/j.antiviral.2019.104564.

Disclosure of potential conflicts of interest

No potential conflicts of interest were disclosed.

References

Cai, Q., Zhao, A., Yuting, Y., Ma, L., Jiao, Z., Zhi, H., Lai, S., Cheng, S., Yang, H., Lu, Y., Siminovitch, K.A., Gao, J., 2014. Efficient production of sTNFRII-gAD fusion protein in large quantity by use of the modified CHO-S cell expression system. PLoS One 9, e111229.
Chen, C., Liu, L., Xiao, Y., Cui, S., Wang, J., Jin, Q., 2018. Structural insight into a human neutralizing antibody against influenza virus H7N9. J. Virol. 92 e01850-01817.
Chen, Z., Wang, J., Bao, L., Guo, L., Zhang, W., Xue, Y., Zhou, H., Xiao, Y., Wang, J., Wu, F., Deng, Y., Qin, C., Jin, Q., 2015. Human monoclonal antibodies targeting the haemagglutinin glycoprotein can neutralize H7N9 influenza virus. Nat. Commun. 6, 6714.
Corti, D., Voss, J., Gamblin, S.J., Codoni, G., Macagno, A., Jarrossay, D., Vachieri, S.G., Pinna, D., Minola, A., Vanzetta, F., Silacci, C., Fernandez-Rodriguez, B.M., Agatic, G., Bianchi, S., Giacchetto-Sasselli, I., Calder, L., Sallusto, F., Collins, P., Haire, L.F., Temperton, N., Langedijk, J.P., Skehel, J.J., Lanzavecchia, A., 2011. A neutralizing antibody selected from plasma cells that binds to group 1 and group 2 influenza A hemagglutinins. Sci. (N. Y.) 333, 850–856.
Cox, F., Kwaks, T., Brandenburg, B., Koldijk, M.H., Klaren, V., Smal, B., Korse, H.J., Geelen, E., Tettero, L., Zuijdgeest, D., 2016. HA antibody-mediated FcγRIIIa activity is both dependent on FcR engagement and interactions between HA and sialic acids. Front. Immunol. 7, 399.
Davies, D.R., Cohen, G.H., 1996. Interactions of protein antigens with antibodies. Proc. Natl. Acad. Sci. U.S.A 93, 7–12.
Ekiert, D.C., Bhabha, G., Elsliger, M.A., Friesen, R.H., Jongeneelen, M., Throsby, M., Goudsmit, J., Wilson, I.A., 2009. Antibody recognition of a highly conserved influenza virus epitope. Sci. (N. Y.) 324, 246–251.
Florian, K., Cox, R.J., 2013. The emergence of H7N9 viruses: a chance to redefine correlates of protection for influenza virus vaccines. Expert Rev. Vaccines 12, 1369–1372.
Fries, L.F., Smith, G.E., Glenn, G.M., 2013. A recombinant viruslike particle influenza A (H7N9) vaccine. N. Engl. J. Med. 369, 2564–2566.
Gao, R., Cao, B., Hu, Y., Feng, Z., Wang, D., Hu, W., Chen, J., Jie, Z., Qiu, H., Xu, K., Xu,

X., Lu, H., Zhu, W., Gao, Z., Xiang, N., Shen, Y., He, Z., Gu, Y., Zhang, Z., Yang, Y., Zhao, X., Zhou, L., Li, X., Zou, S., Zhang, Y., Li, X., Yang, L., Guo, J., Dong, J., Li, Q., Dong, L., Zhu, Y., Bai, T., Wang, S., Hao, P., Yang, W., Zhang, Y., Han, J., Yu, H., Li, D., Gao, G.F., Wu, G., Wang, Y., Yuan, Z., Shu, Y., 2013. Human infection with a novel avian-origin influenza A (H7N9) virus. N. Engl. J. Med. 368, 1888–1897.

Herfst, S., Schrauwen, E.J., Linster, M., Chutinimitkul, S., de Wit, E., Munster, V.J., Sorrell, E.M., Bestebroer, T.M., Burke, D.F., Smith, D.J., Rimmelzwaan, G.F., Osterhaus, A.D., Fouchier, R.A., 2012. Airborne transmission of influenza A/H5N1 virus between ferrets. Sci. (N. Y.) 336, 1534–1541.

Hochleitner, E., Gorny, P.S., Tomer, K., 2000. Mass spectrometric characterization of a discontinuous epitope of the HIV envelope protein HIV-gp120 recognized by the human monoclonal antibody 1331A. J. Immunol. 164, 4156–4161.

Hu, H., Voss, J., Zhang, G., Buchy, P., Zuo, T., Wang, L., Wang, F., Zhou, F., Wang, G., Tsai, C., Calder, L., Gamblin, S.J., Zhang, L., Deubel, V., Zhou, B., Skehel, J.J., Zhou, P., 2012. A human antibody recognizing a conserved epitope of H5 hemagglutinin broadly neutralizes highly pathogenic avian influenza H5N1 viruses. J. Virol. 86, 2978–2989.

Huang, J., Doria-Rose, N.A., Longo, N.S., Laub, L., Lin, C.L., Turk, E., Kang, B.H., Migueles, S.A., Bailer, R.T., Mascola, J.R., Connors, M., 2013. Isolation of human monoclonal antibodies from peripheral blood B cells. Nat. Protoc. 8, 1907–1915.

Huang, K.A., Rijal, P., Jiang, H., Wang, B., Schimanski, L., Dong, T., Liu, Y.M., Chang, P., Iqbal, M., Wang, M.C., Chen, Z., Song, R., Huang, C.C., Yang, J.H., Qi, J., Lin, T.Y., Li, A., Powell, T.J., Jan, J.T., Ma, C., Gao, G.F., Shi, Y., Townsend, A.R., 2019. Structure-function analysis of neutralizing antibodies to H7N9 influenza from naturally infected humans. Nat. Microbiol. 4, 306–315.

Jeyarajah, S., Parker, C.E., Sumner, M.T., Tomer, K.B., 1998. Matrix-assisted laser desorption ionization/mass spectrometry mapping of human immunodeficiency virus-gp120 epitopes recognized by a limited polyclonal antibody. J. Am. Soc. Mass Spectrom. 9, 157–165.

Kallewaard, N.L., Corti, D., Collins, P.J., Neu, U., McAuliffe, J.M., Benjamin, E., Wachter-Rosati, L., Palmer-Hill, F.J., Yuan, A.Q., Walker, P.A., Vorlaender, M.K., Bianchi, S., Guarino, B., De Marco, A., Vanzetta, F., Agatic, G., Foglierini, M., Pinna, D., Fernandez-Rodriguez, B., Fruehwirth, A., Silacci, C., Ogrodowicz, R.W., Martin, S.R., Sallusto, F., Suzich, J.A., Lanzavecchia, A., Zhu, Q., Gamblin, S.J., Skehel, J.J., 2016. Structure and function analysis of an antibody recognizing all influenza a subtypes. Cell 166, 596–608.

Koszalka, P., Tilmanis, D., Hurt, A.C., 2017. Influenza antivirals currently in late-phase clinical trial. Influenza Other Respir. Viruses 11, 240–246.

Lang, S., Xie, J., Zhu, X., Wu, N.C., Lerner, R.A., Wilson, I.A., 2017. Antibody 27F3 broadly targets influenza a group 1 and 2 hemagglutinins through a further variation in VH1-69 antibody orientation on the HA stem. Cell Rep. 20, 2935–2943.

Marjuki, H., Mishin, V.P., Chai, N., Tan, M.W., Newton, E.M., Tegeris, J., Erlandson, K., Willis, M., Jones, J., Davis, T., Stevens, J., Gubareva, L.V., 2016. Human monoclonal antibody 81.39a effectively neutralizes emerging influenza a viruses of group 1 and 2 hemagglutinins. J. Virol. 90, 10446–10458.

Mulligan, M.J., Bernstein, D.I., Patricia, W., Richard, R., Evan, A., Nadine, R., Michelle, D., Stapleton, J.T., Srilatha, E., Paul, S., 2014. Serological responses to an avian influenza A/H7N9 vaccine mixed at the point-of-use with MF59 adjuvant: a randomized clinical trial. JAMA 312, 1409–1419.

Pappas, L., Foglierini, M., Piccoli, L., Kallewaard, N.L., Turrini, F., Silacci, C., Fernandez-Rodriguez, B., Agatic, G., Giacchetto-Sasselli, I., Pellicciotta, G., Sallusto, F., Zhu, Q., Vicenzi, E., Corti, D., Lanzavecchia, A., 2014. Rapid development of broadly influenza neutralizing antibodies through redundant mutations. Nature 516, 418–422.

Prabakaran, M., Prabhu, N., He, F., Hongliang, Q., Ho, H.T., Qiang, J., Meng, T., Goutama, M., Kwang, J., 2009. Combination therapy using chimeric monoclonal antibodies protects mice from lethal H5N1 infection and prevents formation of escape mutants. PLoS One 4, e5672.

Quan, C., Shi, W., Yang, Y., Yang, Y., Liu, X., Xu, W., Li, H., Li, J., Wang, Q., Tong, Z., Wong, G., Zhang, C., Ma, S., Ma, Z., Fu, G., Zhang, Z., Huang, Y., Song, H., Yang, L., Liu, W.J., Liu, Y., Liu, W., Gao, G.F., Bi, Y., 2018. New threats from H7N9 influenza virus: spread and evolution of high- and low-pathogenicity variants with high genomic diversity in wave five. J. Virol. 92 e00301-00318.

Reed, L.J., Muench, H., 1938. A simple method of estimating fifty percent endpoints. Am. J. Epidemiol. 27, 493–497.

Rogers, G.N., Paulson, J.C., Daniels, R.S., Skehel, J.J., Wilson, I.A., Wiley, D.C., 1983. Single amino acid substitutions in influenza haemagglutinin change receptor binding specificity. Nature 304, 76–78.

Schmeisser, F., Vasudevan, A., Verma, S., Wang, W., Alvarado, E., Weiss, C., Atukorale, V., Meseda, C., Weir, J.P., 2015. Antibodies to antigenic site A of influenza H7 hemagglutinin provide protection against H7N9 challenge. PLoS One 10, e0117108.

Shi, Y., Zhang, W., Wang, F., Qi, J., Wu, Y., Song, H., Gao, F., Bi, Y., Zhang, Y., Fan, Z., Qin, C., Sun, H., Liu, J., Haywood, J., Liu, W., Gong, W., Wang, D., Shu, Y., Wang, Y., Yan, J., Gao, G.F., 2013. Structures and receptor binding of hemagglutinins from human-infecting H7N9 influenza viruses. Sci. (N. Y.) 342, 243–247.

Smith, K., Garman, L., Wrammert, J., Zheng, N.Y., Capra, J.D., Ahmed, R., Wilson, P.C., 2009. Rapid generation of fully human monoclonal antibodies specific to a vaccinating antigen. Nat. Protoc. 4, 372–384.

Stadlbauer, D., Rajabhathor, A., Amanat, F., Kaplan, D., Masud, A., Treanor, J.J., Izikson, R., Cox, M.M., Nachbagauer, R., Krammer, F., 2017. Vaccination with a recombinant H7 hemagglutinin-based influenza virus vaccine induces broadly reactive antibodies in humans. mSphere 2 e00502-00517.

Subbarao, K., 2018. Avian influenza H7N9 viruses: a rare second warning. Cell Res. 28, 1.

Sui, J., Hwang, W.C., Perez, S., Wei, G., Aird, D., Chen, L.M., Santelli, E., Stec, B., Cadwell, G., Ali, M., Wan, H., Murakami, A., Yammanuru, A., Han, T., Cox, N.J., Bankston, L.A., Donis, R.O., Liddington, R.C., Marasco, W.A., 2009. Structural and functional bases for broad-spectrum neutralization of avian and human influenza A viruses. Nat. Struct. Mol. Biol. 16, 265–273.

Tan, G.S., Leon, P.E., Albrecht, R.A., Margine, I., Hirsh, A., Bahl, J., Krammer, F., 2016. Broadly-Reactive neutralizing and non-neutralizing antibodies directed against the H7 influenza virus hemagglutinin reveal divergent mechanisms of protection. PLoS Pathog. 12, e1005578.

Terajima, M., Cruz, J., Co, M.D., Lee, J.H., Kaur, K., Wrammert, J., Wilson, P.C., Ennis, F.A., 2011. Complement-dependent lysis of influenza a virus-infected cells by broadly cross-reactive human monoclonal antibodies. J. Virol. 85, 13463–13467.

Tharakaraman, K., Subramanian, V., Cain, D., Sasisekharan, V., Sasisekharan, R., 2014. Broadly neutralizing influenza hemagglutinin stem-specific antibody CR8020 targets residues that are prone to escape due to host selection pressure. Cell Host Microbe 15, 644–651.

Tharakaraman, K., Subramanian, V., Viswanathan, K., Sloan, S., Yen, H.L., Barnard, D.L., Leung, Y.H., Szretter, K.J., Koch, T.J., Delaney, J.C., Babcock, G.J., Wogan, G.N., Sasisekharan, R., Shriver, Z., 2015. A broadly neutralizing human monoclonal antibody is effective against H7N9. Proc. Natl. Acad. Sci. U. S. A. 112, 10890–10895.

Tom, R., Bisson, L., Durocher, Y., 2008. Transfection of HEK293-EBNA1 cells in suspension with linear PEI for production of recombinant proteins. Cold Spring Harb. Protoc. 2008 pdb prot4977.

Vanderven, H.A., Jegaskanda, S., Wheatley, A.K., Kent, S.J., 2017. Antibody-dependent cellular cytotoxicity and influenza virus. Curr. Opin. Virol. 22, 89–96.

Wang, J., Chen, Z., Bao, L., Zhang, W., Xue, Y., Pang, X., Zhang, X., Qin, C., Jin, Q., 2015. Characterization of two human monoclonal antibodies neutralizing influenza a H7N9 viruses. J. Virol. 89, 9115–9118.

Watanabe, T., Watanabe, S., Maher, E.A., Neumann, G., Kawaoka, Y., 2014. Pandemic potential of avian influenza A (H7N9) viruses. Trends Microbiol. 22, 623–631.

Webster, R.G., Laver, W.G., 1980. Determination of the number of nonoverlapping antigenic areas on Hong Kong (H3N2) influenza virus hemagglutinin with monoclonal antibodies and the selection of variants with potential epidemiological significance. Virology 104, 139–148.

Wilson, I.A., Skehel, J.J., Wiley, D.C., 1981. Structure of the haemagglutinin membrane glycoprotein of influenza virus at 3 A resolution. Nature 289, 366–373.

Wu, Y., Bi, Y., Vavricka, C., Sun, X., Zhang, Y., Gao, F., Zhao, M., Xiao, H., Qin, C., He, J., 2013. Characterization of two distinct neuraminidases from avian-origin human-infecting H7N9 influenza viruses. Cell Res. 23, 1347–1355.

Wu, Y., Cho, M., Shore, D., Song, M., Choi, J., Jiang, T., Deng, Y.Q., Bourgeois, M., Almli, L., Yang, H., Chen, L.M., Shi, Y., Qi, J., Li, A., Yi, K.S., Chang, M., Bae, J.S., Lee, H., Shin, J., Stevens, J., Hong, S., Qin, C.F., Gao, G.F., Chang, S.J., Donis, R.O., 2015. A potent broad-spectrum protective human monoclonal antibody crosslinking two haemagglutinin monomers of influenza A virus. Nat. Commun. 6, 7708.

Xiong, X., Corti, D., Liu, J., Pinna, D., Foglierini, M., Calder, L.J., Martin, S.R., Lin, Y.P., Walker, P.A., Collins, P.J., Monne, I., Suguitan Jr., A.L., Santos, C., Temperton, N.J., Subbarao, K., Lanzavecchia, A., Gamblin, S.J., Skehel, J.J., 2015. Structures of complexes formed by H5 influenza hemagglutinin with a potent broadly neutralizing human monoclonal antibody. Proc. Natl. Acad. Sci. U. S. A. 112, 9430–9435.

Xiong, X., Martin, S.R., Haire, L.F., Wharton, S.A., Daniels, R.S., Bennett, M.S., McCauley, J.W., Collins, P.J., Walker, P.A., Skehel, J.J., Gamblin, S.J., 2013. Receptor binding by an H7N9 influenza virus from humans. Nature 499, 496–499.

Xu, R., de Vries, R.P., Zhu, X., Nycholat, C.M., McBride, R., Yu, W., Paulson, J.C., Wilson, I.A., 2013. Preferential recognition of avian-like receptors in human influenza A H7N9 viruses. Sci. (N. Y.) 342, 1230–1235.

Yamayoshi, S., Uraki, R., Ito, M., Kiso, M., Nakatsu, S., Yasuhara, A., Oishi, K., Sasaki, T., Ikuta, K., Kawaoka, Y., 2017. A broadly reactive human anti-hemagglutinin stem monoclonal antibody that inhibits influenza a virus particle release. EBioMedicine 17, 182–191.

Yen, H.L., McKimm-Breschkin, J.L., Choy, K.T., Wong, D.D.Y., Cheung, P.P.H., Zhou, J., Ng, I.H., Zhu, H., Webby, R.J., Guan, Y., Webster, R.G., Peiris, J.S.M., 2013. Resistance to neuraminidase inhibitors conferred by an R292K mutation in a human influenza virus H7N9 isolate can be masked by a mixed R/K viral population. mBio 4 e00396-00313.

Yu, F., Song, H., Wu, Y., Chang, S.Y., Wang, L., Li, W., Hong, B., Xia, S., Wang, C., Khurana, S., Feng, Y., Wang, Y., Sun, Z., He, B., Hou, D., Manischewitz, J., King, L.R., Song, Y., Min, J.Y., Golding, H., Ji, X., Lu, L., Jiang, S., Dimitrov, D.S., Ying, T., 2017. A potent germline-like human monoclonal antibody targets a pH-sensitive epitope on H7N9 influenza hemagglutinin. Cell Host Microbe 22, 471–483.